

Kinetics of surface roughening via pit growth during the oxidation of the basal plane of graphite. II. Theory and simulation

T. Pakula, A. Tracz,^{a)} G. Wegner, and J. P. Rabe^{b)}

Max-Planck-Institut für Polymerforschung, Postfach 3148, D-55021 Mainz, Germany

(Received 8 March 1993; accepted 19 July 1993)

Analytical expressions for the description of the oxidation kinetics of the basal planes of the graphite surface are proposed. They are developed from an ansatz that extends former theories of phase transformations by nucleation and growth to multilayer systems in which the kinetics of transformation in subsequent layers is recurrently related. The results from analytical theory are compared with computer simulations obtained for an adequate model. Correspondence of these results to the structural changes observed in the oxidation of the graphite surface, as revealed by scanning tunneling microscopy, is discussed.

INTRODUCTION

The oxidation of the basal plane of highly oriented pyrolytic graphite (HOPG) has been studied by scanning tunneling microscopy (STM).¹ It was experimentally observed that the oxidation of basal planes of the graphite leads to the removal of monoatomic carbon layers from the graphite surface, layer by layer, via nucleation and growth of circular pits on the exposed surface. Two types of samples differing in the kinetics of nucleation have been distinguished (a) with nuclei that start to grow simultaneously at the beginning of the oxidation leading to pits of uniform diameter at the initial stages of the process and (b) with nuclei that become active sporadically, which leads to pits with a broad distribution of diameters.

The phenomena observed have many analogies and similar processes have been treated theoretically by many authors, a long time ago.²⁻⁷ Theories have been developed for various phenomena such as crystallization from the melt, surface corrosion or propagation of waves on water surfaces. They rely on the same model of isotropically growing objects nucleated according to various kinetic schemes, which lead to different time-laws by which the system is transformed from one state to another, e.g., from the amorphous to the crystalline state. The most interesting ingredient of all theories is the handling of the effect of encroachment of the growing objects leading to a slow down of the overall transformation rate in comparison to the rate one would expect without encroachment.

In this paper a model to describe the oxidation kinetics of the graphite surface is proposed. The model extends the application of former theories to multilayer systems in which the kinetics of transformation in subsequent layers is recurrently related. The results of the analytical theory are compared with a computer simulation of an adequate model. Correspondence of these results to the experimental observations reported in a separate paper¹ is discussed.

THEORETICAL MODEL

Consider a monoatomic uniform planar layer of carbon atoms which, when undergoing oxidation, disappear from the layer as a gaseous product. If the oxidation takes place by nucleation and growth, circular pits will expand throughout the layer encroaching at later stages of the process. The nontransformed fraction S of the layer at time t is related to the potentially transformed area E (with ignored overlap of the pits) by the relation

$$S(t) = \exp[-E(t)]. \quad (1)$$

This relation is deduced from the Poisson distribution² and is known as the Avrami equation,⁴ which is usually expressed in the form $S = \exp(-Kt^\alpha)$.

The potentially transformed area E , with ignored encroachment, depends on the nucleation kinetics, dimensionality of the system, and on the radial growth rate v . In the case of two-dimensional growth of pits, being of interest in this paper, E is just calculated as a sum of areas of circular pits which appear from the beginning of the process. Two kinds of nucleation kinetics are of interest (1) the nuclei are present in the system and become active instantaneously at the beginning of the process or (2) they may appear progressively during the course of the process.

For the two cases of instantaneous and sporadic nucleation E can be expressed as⁷

$$E(t) = \pi N v^2 t^2, \quad (2)$$

where N is the number of instantaneous nuclei per unit surface, and

$$E(t) = \pi n v^2 \int_0^t (t-\tau)^2 d\tau = \pi n v^2 t^3/3, \quad (3)$$

where n is the number of nuclei which appear per unit time and unit surface, respectively.

This result serves to describe the initial stages of the oxidation process of the basal plane of graphite if one starts with a uniform surface formed by a single basal plane. As the growth of pits in the first layer proceeds, the new surface of the next layer underneath is exposed on which new pits can be nucleated contributing to the overall rate of oxidation. In this way the kinetics of oxidation of the i th

^{a)}Present address: Polish Academy of Sciences, Center of Molecular and Macromolecular Studies, Sienkiewicza 112, 90-363 Lodz, Poland.

^{b)}Present address: J. Gutenberg-Universität Mainz, Institut für Physikalische Chemie, Jakob-Welder-Weg 11, D-55099 Mainz, Germany.

layer will depend on the growth of pits in the $i-1$ layer. In order to consider this effect we have again to distinguish various nucleation mechanisms in the newly exposed layers. Two probable cases may be of interest (1) the nucleation occurs at intrinsic defects which will become active as soon as they are exposed and (2) the nucleation occurs sporadically on the exposed surface. In the first case the nucleation rate n_i will be given by the density of defects per unit layer area and by the rate of exposure of the layer, which depends on the kinetics of disappearance of the former layer. In the second case the nucleation rate will depend on the probability to form a nucleus and on the exposed layer area. For the two cases we can write

$$n_i(t) = N \frac{dS_{i-1}(t)}{dt} \quad (4)$$

and

$$n_i(t) = n [1 - S_{i-1}(t)], \quad (5)$$

respectively, where N [as in Eq. (2)] is the density of defects leading to instantaneous nucleation of pits when the defect becomes exposed and n [as in Eq. (3)] is the rate of sporadic nucleation per unit area and unit time. Considering the circular growth with a radial rate v and taking encroachment of pits into account we can write

$$S_i(t) = \exp \left[-\pi v^2 \int_0^t n_i(\tau) (t-\tau)^2 d\tau \right] \quad (6)$$

which for intrinsic and sporadic nuclei assumes the form

$$S_i(t) = \exp \left[-\pi N v^2 \int_0^t \left[\frac{dS_{i-1}(\tau)}{d\tau} \right] (t-\tau)^2 d\tau \right] \quad (7)$$

and

$$S_i(t) = \exp \left[-\pi n v^2 \int_0^t S_{i-1}(\tau) (t-\tau)^2 d\tau \right], \quad (8)$$

respectively.

These recurrent relations allow to calculate the kinetics of multilayer oxidation numerically. Figures 1 and 2 show the kinetic behavior of multilayer oxidation for two cases differing in nucleation nature, i.e., for instantaneous and sporadic nucleation, respectively. Figures 1(a) and 2(a) show the time dependencies of the nontransformed fraction $S_i(t)$ of subsequent layers. In Figs. 1(b) and 2(b) the transformation rate for individual layers $-dS_i(t)/dt$ and the overall transformation rate

$$K(t) = - \sum dS_i(t)/dt \quad (9)$$

are presented as a function of time. The value of $-dS_i(t)/dt$ characterizes the length of pit edges for individual layers, whereas, $K(t)$ is proportional to the length of all pit edges at the exposed surface. In this way, both the behavior of subsequent layers and of the global sample are characterized. The two types of nucleation lead to a qualitatively rather similar global behavior. The main differences are observed at the initial stages of oxidation where in the case of instantaneous nucleation the oxidation rate increases

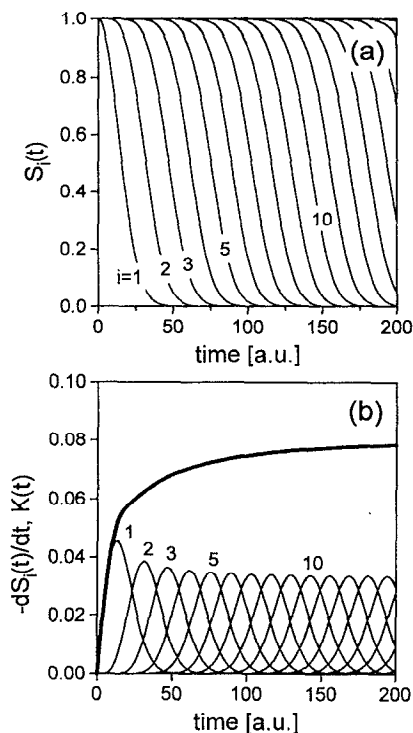


FIG. 1. The kinetics of oxidation of a multilayer surface in the case of instantaneous nucleation on intrinsic defects. (a) Time dependence of the nontransformed area of subsequent layers. (b) Time dependence of the transformation rate of subsequent layers and of the overall transformation rate (thick solid line). Nucleation density $N=0.0009$ per unit surface and the growth rate $v=1$.

monotonously while in the other case a rapid rate increase is observed at the very beginning followed by periodic rate changes of the amplitude decreasing with time. When several layers are removed from the surface the global rate of oxidation approaches a plateau in both cases independent of nucleation kinetics. At this stage the kinetics of removal of subsequent layers becomes stationary. At longer times the difference between the two cases considered consists first of all in a difference in the time of the effective oxidation of individual layers in comparison to the time lag in the oxidation of subsequent layers. When the nucleation occurs instantaneously the kinetic curves are broader than in the other case. This has the consequence that a different number of layers is exposed simultaneously at a given time. In the case of instantaneous nucleation the number of layers exposed at later stages of oxidation is 6, whereas, in the case of the sporadic nucleation only 4 layers can simultaneously be seen at the surface. This effect could eventually help to distinguish the nature of the nucleation process experimentally.

It is interesting to prove how the parameters of the process, i.e., the growth rate and nucleation density influence the global kinetics. Time dependencies of global oxidation rates at various nucleation densities for the two cases considered are shown in Fig. 3, within the time interval necessary to remove 15 layers from the surface. It is seen that the rate of oxidation increases with nucleation density in both cases and consequently the time to remove

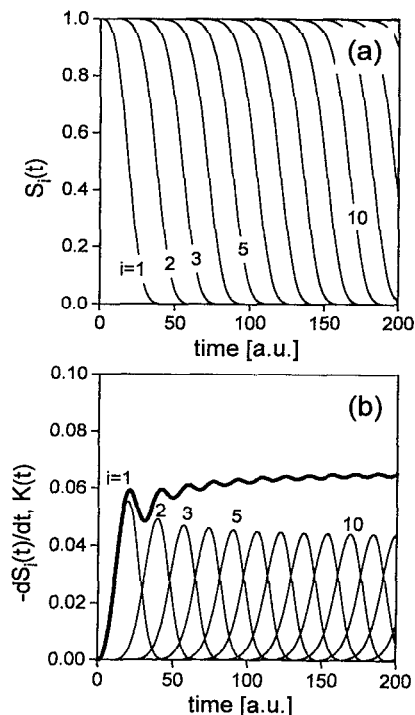


FIG. 2. The kinetics of oxidation of a multilayer surface in the case of sporadic nucleation. (a) Time dependence of the nontransformed area of subsequent layers. (b) Time dependence of the transformation rate of subsequent layers and of the overall transformation rate (thick solid line). Nucleation rate $n=0.0001$ per unit time and unit surface and the growth rate $v=1$.

a given number of layers decreases. It is worth mentioning that the rate $K(t)$ reached at the removal of the i th layer ($i=15$) fits well to the hyperbolic dependence $K_{i=15} \propto t^{-1}$, as illustrated in Fig. 3. It has also been established that a master curve can be obtained if the dependencies are plotted in the coordinates $K(t)/(vN^{1/2})$ vs $tvN^{1/2}$ for the instantaneous nucleation and as $K(t)/(v^{2/3}n^{1/3})$ vs $tv^{2/3}n^{1/3}$, where n is the nucleation rate, for the sporadic nucleation. This allows to deduce the following dependencies:

(1) the overall rate of oxidation at long time is

$$K \propto vN^{1/2} \quad (10)$$

and (2) the time to reach a certain conversion state is

$$t_i \propto v^{-1}N^{-1/2} \quad (11)$$

in the case of instantaneous nucleation. If the nucleation is sporadic the dependencies are

$$K \propto v^{2/3}n^{1/3}, \quad (12)$$

$$t_i \propto v^{-2/3}n^{-1/3}. \quad (13)$$

SIMULATION

Computer simulations have been performed on systems which correspond to the models presented above. Systems of parallel layers consisting of densely packed discrete elements on a quadratic lattice of the size 500×600 elements in each layer have been considered. The process of

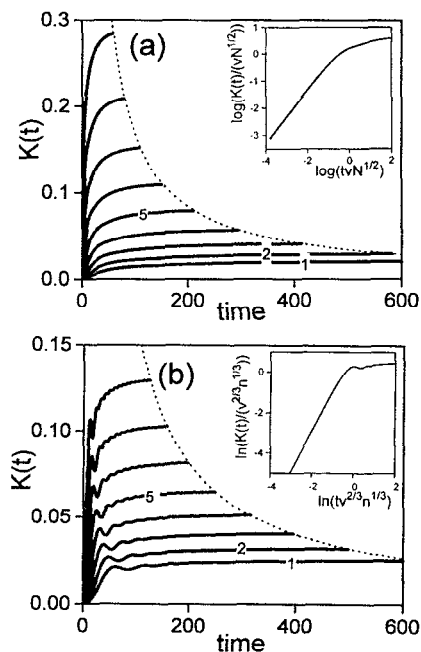


FIG. 3. The transformation rate as a function of time for various nucleation densities (a) instantaneous nucleation (curve 1 is calculated for the nucleation density $N=0.00002$, for each subsequent curve the nucleation density is higher by factor 2) and (b) sporadic nucleation (curve 1 is calculated for the nucleation rate $n=0.000002$, for each subsequent curve the nucleation rate is increased by a factor of 2). Insertions show master curves plotted in coordinates characteristic for each nucleation type. The broken lines indicate dependencies on global oxidation rate and time at the same conversion (15 layers are completely removed from the surface) but variable nucleation densities.

oxidation is modeled by nucleation of pits of the size of one element and subsequent isotropic growth of the pits with constant linear rate. In order to avoid boundary effects periodic boundary conditions within each layer have been assumed. As before two kinds of the nucleation have been considered.

(1) The nucleation occurs at intrinsic defects randomly distributed in the system before the oxidation. In the first layer, the defects become active nuclei at $t=0$ and in other layers at the moment they become exposed.

(2) The sporadic nucleation consists in random generation of single element vacancies, in any one of the exposed layers, at a given rate.

The simulation allows a direct observation of the surface structures which develop during oxidation of multilayer systems. Two series of pictures, at various stages of the process, related to the two different nucleation modes are shown in Figs. 4 and 5. The characteristic features can easily be noticed. In the case of nucleation from intrinsic defects all nuclei in the first layer start to grow at the same time $t=0$, consequently the pits are of the same radius [Fig. 4(a)]. In the next layer the pits start to grow at edges of pits in the former layer so that the pits in subsequent layers are tangential (if locally this is not influenced by the encroachment).

In the case of sporadic nucleation the sizes of pits are broadly distributed already in the first layer [Fig. 5(a)].

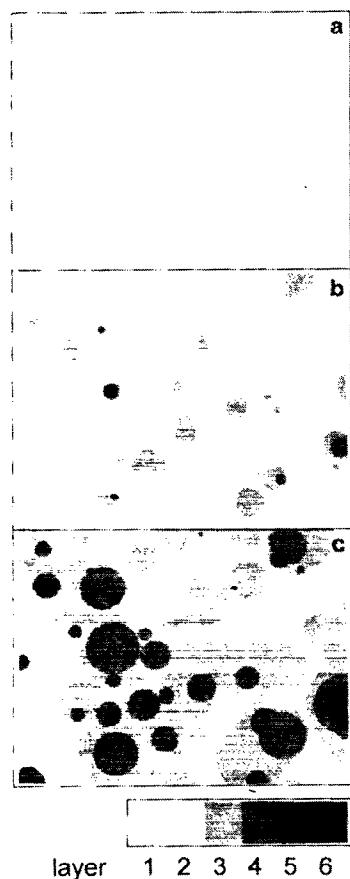


FIG. 4. Illustration of the development of pits during simulated oxidation of a multilayer system with instantaneous nuclei (a) $t=10$; (b) $t=25$; and (c) $t=50$.

The positions of pits in subsequent layers do not have the correlation observed in the former case. In both cases, at later stages of conversion the structure of the surface becomes almost stationary. The difference in the number of layers exposed in the systems with different kinds of nucleation is seen in agreement with the effect suggested from analytical treatment of the model. A comparison of the simulated surfaces at later stages (the two first layers are completely removed from the surface) for the two nucleation types is shown in Fig. 6. In the case of sporadic nucleation usually 4 layers can be seen simultaneously [Fig. 6(b)], whereas in the other case 6 layers form the surface at later stages of the process [Fig. 6(a)].

The kinetic features of the simulated systems are characterized quantitatively by the same quantities as considered for the analytical model in Figs. 7 and 8 (compare with Figs. 1 and 2). The rate of transformation of individual layers is determined from the length of edges of pits formed in each layer.

DISCUSSION

The results presented above show that the agreement between the analytical expressions and the computer simulation is qualitatively very good. An important difference between simulated and theoretical results can, however, be

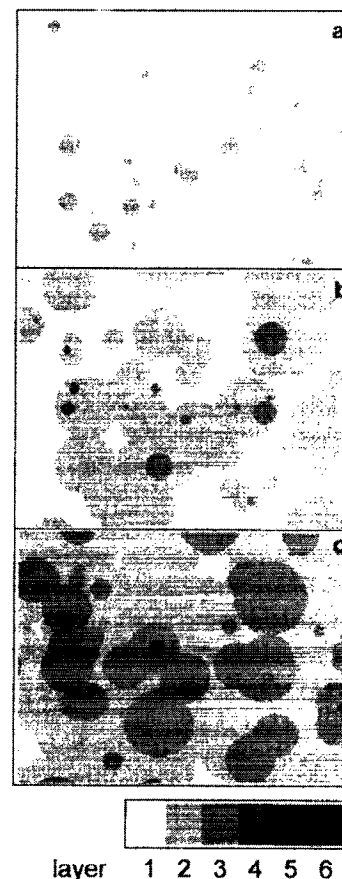


FIG. 5. Illustration of the development of pits during simulated oxidation of a multilayer system with sporadic nucleation (a) $t=15$; (b) $t=40$; and (c) $t=80$.

noticed at longer reaction times. Whereas the analytical theory predicts that at longer times the rate of disappearance of subsequent layers become identical the simulation indicates a different behavior. In the latter case the dependencies for individual layers become broader with increasing time. This has important consequences considering changes in the structure of the oxidized surface. In contrast to the theoretical prediction the roughness of the system increases with time, i.e., more and more subsequent layers contribute simultaneously to the exposed surface. It also means that in the simulated surfaces after long time deeper pits can be formed than the analytical theory would predict. This discrepancy can be a result of fluctuations in the distributions of nuclei in subsequent layers of the simulated systems.

In spite of this structural difference the global kinetic characteristics obtained from the simulated systems agree well with the theoretical model. The time dependencies of the overall rates as obtained from the theory and from the simulated systems, with the same values of nucleation densities and growth rates, are directly compared in Fig. 9.

In Fig. 10 the surface morphology of oxidized HOPG samples of type A and type B at initial and later oxidation stages in air at 670 °C are shown (see also Figs. 2, 3, and 6 in Ref. 1). A comparison of Fig. 10 with Figs. 4 and 5

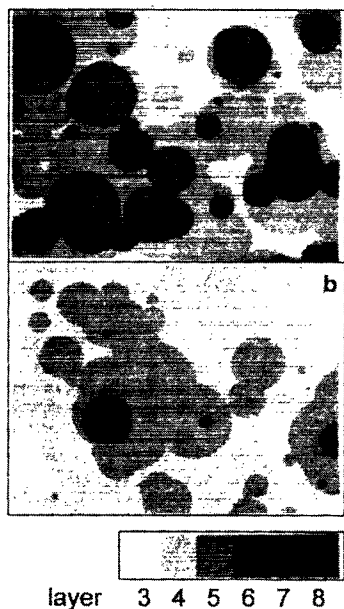


FIG. 6. A comparison of simulated surfaces at a longer time of oxidation for (a) instantaneous and (b) sporadic nucleation. Pictures are taken after the two first layers are completely removed from the surface.

indicates that the effects observed on the simulated surfaces correspond well to the surface morphology of HOPG after a real oxidation process. Both for real and simulated surface morphologies the same characteristic features of multilevel terraced structure can be seen, i.e., smaller pits grow within bigger ones and remains of the upper layers form

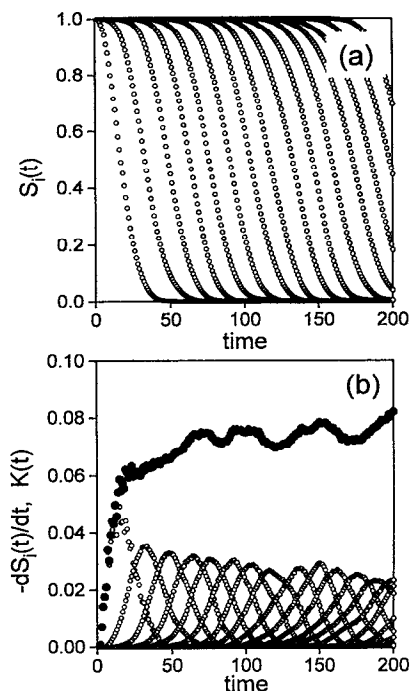


FIG. 7. Computer simulated kinetics of oxidation in the case of instantaneous nucleation. The quantities determined and the parameters correspond to these used in Fig. 1.

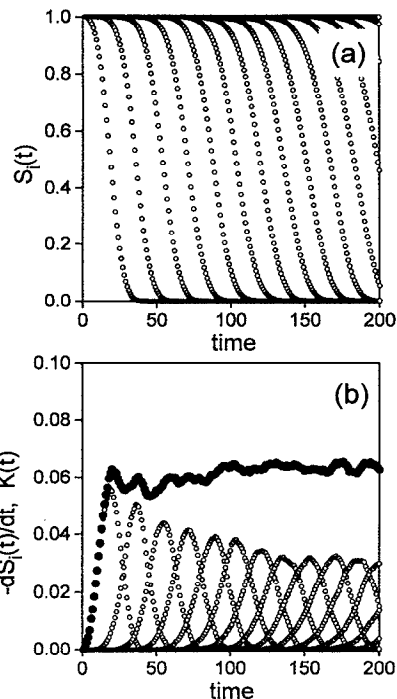


FIG. 8. Computer simulated kinetics of oxidation in the case of sporadic nucleation. The quantities determined and the parameters correspond to these used in Fig. 2.

pieces with concave curved edges. The differences in surface structure caused by the two different nucleation types considered in simulation correspond also to differences observed in samples of type A and B. The simulated surface

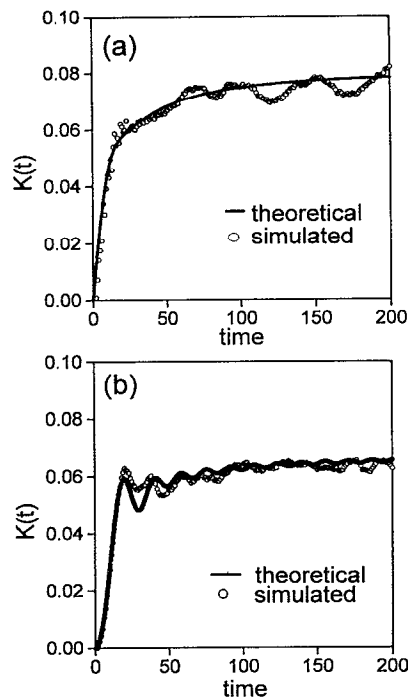


FIG. 9. Comparison between theoretical and computer simulated time dependencies of the overall oxidation rate for the two types of nucleation (a) instantaneous nucleation and (b) sporadic nucleation.

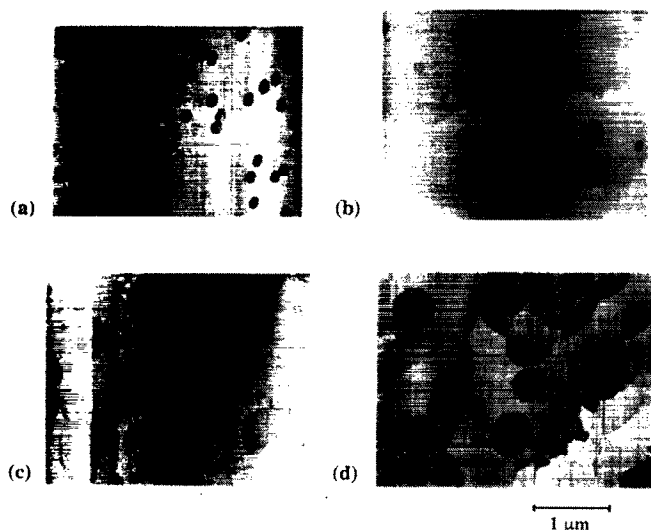


FIG. 10. Oxidized surfaces of graphite as observed by scanning tunneling microscopy at (a) and (b) initial and (c) and (d) later stages of oxidation for two types of samples with instantaneous nucleation (a) and (c) and sporadic nucleation (b) and (d).

in the case of instantaneous nucleation (Fig. 4) corresponds to the surface of samples of type A for which the simultaneous growth of pits of uniform size was observed at initial stages of oxidation [compare Figs. 4(a) and 10(a)]. At later stages of oxidation smaller pits growing tangentially inside bigger ones have been observed [Fig. 10(c)] which corresponds to structures presented in Figs. 4(b) and 4(c). In the same way the simulated surface structures in Fig. 5 correspond to HOPG surfaces shown in Figs. 10(b) and 10(d) (samples of type B) illustrating a distribution of pit sizes at the beginning of oxidation and pits nucleated nontangentially within other already existing pits [see also Fig. 7(b) in Ref. 1]. It is interesting to compare the number of carbon atom levels exposed at later oxidation stages as observed in real process with the number of layers predicted by the analytical expressions and in the simulation. In the case of samples of type A the num-

ber of levels observed was 6 on average. This is in agreement with the theoretical result obtained under the assumption of instantaneous nucleation. In the case of samples of type B 5 levels can simultaneously be seen at later stages of oxidation of HOPG. This number is lower than theoretical prediction for instantaneous nucleation (6 levels) and higher than the prediction for sporadic nucleation (4 levels). This can be interpreted as an indication that in the case of samples of type B the growth of pits occurs via nucleation process which is a mixture of sporadic and instantaneous nucleation. This supports the hypothesis about the presence of defects of different nature in samples of type B as postulated elsewhere.¹

An important property of the surface roughening via pit growth, predicted by the analytical model and confirmed by the simulation, is the tendency of leveling off of the total length of edges at longer oxidation times. The dependencies given by master curves, shown in Fig. 3, will be useful to determine conditions of preparation of graphite samples with a controlled amount of reactive edge carbon atoms which may be further functionalized. It is interesting to note that a considerable ratio of reactive edge atoms to nonreactive basal atoms can be achieved already when the third layer becomes exposed [see Figs. 1(b), 2(b), 6(b), and 7(b)] i.e., at a degree of conversion at which the surface roughness is still very small and the surface can be considered as flat on the nanometer scale.

ACKNOWLEDGMENT

This work has been supported by ESPRIT Project 7282 (TOPFIT).

¹A. Tracz, G. Wegner, and J. P. Rabe, *Langmuir* (in press).

²S. D. Poisson; *Recherches sur la Probabilite des Jugements en matieres criminelle et en matiere civile* (Bachelier, Paris, 1837), p. 206.

³A. N. Kolmogoroff, *Izv. Akad. Nauk SSSR, Ser. Math.* **1**, 335 (1937).

⁴M. Avrami, *J. Chem. Phys.* **7**, 1103 (1939).

⁵U. R. Evans, *Trans. Faraday Soc.* **41**, 365 (1945).

⁶M. C. Tobin, *J. Polym. Sci. Polym. Phys. Ed.* **12**, 399 (1974).

⁷V. Raghavan and M. Cohen, in *Solid-State Phase Transitions*, Vol. 5 in *Treatise on Solid State Chemistry*, edited by N. B. Hannay (Plenum, New York, 1975), p. 67.